Oligonucleotide Studies of Sequence-Specific Binding of Chromomycin A_3 to DNA†

Chengdi Liu and Fu-Ming Chen*

Department of Chemistry, Tennessee State University, Nashville, Tennessee 37209-1561

Received September 22, 1993; Revised Manuscript Received November 11, 1993®

ABSTRACT: Systematic kinetic, equilibrium binding, melting, and electrophoretic studies were carried out with oligonucleotides to determine the sequence specificities of chromomycin A_3 (CHR) binding to DNA at the self-complementary tetranucleotide level. Decamers of the forms d(GTA-XGCY-TAC) and d(GTA-XCGY-TAC), with X, Y = A, G, C, or T, were used for this purpose. Results indicate that the binding preferences for CHR are in the order -GGCC- > -CGCG- > -GCGC-, -CCGG- > -AGCT- > -ACGT-, -TGCA- > -TCGA-. Detergent-induced drug dissociation studies revealed that CHR dissociates very slowly from both -GGCC- and -CGCG- sequences, with the former being measurably slower than the latter which in turn is at least an order of magnitude slower than the rest of the sequences. Thermal denaturation measurements indicate that the binding of CHR stabilizes the DNA duplex, with -GGCC- and -CGCG- exhibiting the largest effects. Results of gel electrophoretic retardation experiments support our general findings on the relative binding order. Our experimental results support earlier NMR findings by other researchers implicating the preference of aureolic acid drugs at the 5′GC3′ step and further reveal significant modulations by the adjacent base pairs. Attempts were made to rationalize our results with the known detailed structural information from NMR studies.

Chromycin A_3 (CHR), mithramycin (MTR), and olivomycin are three closely related antitumor antibiotics of the aureolic acid class which contain an aglycon chromophore with di- and trisaccharide (2,6-dideoxyhexapyranose) side chains attached on opposite sides. The antitumor activity of these drugs is believed to be the consequence of the ability to bind to duplex DNA which results in the inhibition of DNA-directed RNA synthesis. These drugs are known to be guanine-specific (Ward et al., 1965; Kaziro & Kamiyama, 1967), and their DNA binding requires the presence of divalent cations such as magnesium (Behr & Hartmann, 1965; Goldberg & Freeman, 1971). Footprinting studies (Van Dyke & Dervan, 1983; Fox & Howarth, 1985; Cons & Fox, 1989a,b; Stankus et al., 1992) have confirmed their guanine specificity and further indicated that the binding sites are at least three base pairs long. The presence of two contiguous G·C base pairs is necessary but not sufficient by themselves for strong DNA binding of these aureolic acids. Consequently, their affinities appear to be modulated by flanking sequences.

Earlier physicochemical studies had produced contradictory conclusions on the DNA binding mode of these drugs. The general consensus was that nonintercalative binding occurred at the minor groove because CHR and MTR fail to affect some properties of DNA such as its sedimentation coefficient and viscosity (Goldberg & Friedman, 1971; Kersten et al., 1966) and do not significantly affect the supercoiling of DNA (Waring, 1970). Conversely, other reports indicated an intercalative (Prasad & Nayak, 1976; Dasgupta et al., 1979) or major groove (Keniry et al., 1987) binding mode. Recent definitive NMR studies on the CHR–d(TTGGCCAA) (Gao & Patel, 1989; Gao et al., 1992) and CHR–d(AAGGCCTT) (Gao & Patel, 1990) complexes in Mg^{2+}-containing solutions have established unequivocally that CHR binds as a Mg^{2+}-coordinated dimer at the minor groove of the central GGCC segment of the duplex and have revealed the structural basis for the sequence specificity at the 5′GC3′ step. The minor groove drug dimer binding model and sequence preference of GC over CG were subsequently verified by other NMR studies (Banville et al., 1990).

Although footprinting experiments have provided some sequence preference information on these drugs, no systematic investigation using other techniques to determine sequence specificity has been performed to date. Our earlier studies with polynucleotides have indicated some sequence or conformational effects on their DNA binding. For example, poly(dA-dG)·poly(dC-dT) exhibits stronger affinity for CHR and MTR than its sequence isomer poly(dA-dC)·poly(dG-dT) (Sarker & Chen, 1989). The detailed structural information available on the binding to -GGCC- (Gao et al., 1992) and -CGCG- sequences (Sastry & Patel, 1993) has provided considerable insights into the structure and dynamics of aureolic acid–DNA interactions. Hence, a systematic study on the specificities to other sequences via synthetic oligonucleotides would be of value. As a first step in elucidating the tetranucleotide sequence specificity of aureolic acids, CHR binding and kinetic studies have been carried out on self-complementary decamers of the form d(GTA-XGCY-TAC) and d(GTA-XCGY-TAC). The results are reported herein as well as our plausible explanations which correlate our findings with the detailed structural information available.

MATERIALS AND METHODS

Oligonucleotides were purchased from Integrated DNA Technologies, Coralville, IA, and used without further purification. All experiments were carried out in 10 mM *N*-(2-hydroxyethyl)piperazine-*N*′-3-propanesulfonic acid (HEPPS) buffer solutions of pH 8 containing 0.1 M NaCl and 1 mM $MgCl_2$. Concentrations of these oligomers (per nucleotide) were determined by measuring the absorbance at 260 nm after melting, with use of extinction coefficients obtained via nearest-neighbor approximation using mono- and dinucleotide

† Supported by USPHS Grant CA-42682 and by a subproject of Minority Biomedical Research Support (MBRS) Grant S06GM0892.
® Abstract published in *Advance ACS Abstracts,* January 15, 1994.

0006-2960/94/0433-1419$04.50/0

values tabulated in Fasman (1975). CHR was purchased from Sigma, and the extinction coefficient of 10 000 cm^{-1} M^{-1} at 406 nm was used for its concentration determination. Absorption spectra were measured with a Cary 1E spectrophotometric system. Spectral titrations were carried out at 25 °C by starting with a drug solution followed by progressive additions of the oligomer stock. Absorbance differences between 400 and 440 nm were used to obtain binding isotherms and Scatchard plots. Kinetic measurements by means of absorbance monitoring were carried out using the Cary 1E temperature controller and stirrer accessory. Time-dependent absorbance changes were monitored at 440 nm for the association experiments and at 340 nm for the 1% sodium dodecyl sulfate (SDS)-induced dissociation experiments. Thermal denaturation experiments of 40 μM oligomer in the absence and in the presence of 5 μM CHR were carried out with 1-cm semimicro cells by monitoring the absorbance at 275 nm. A heating rate of 0.5 °C/min was maintained by the temperature controller accessory. Numerical differentiations were performed to obtian differential melting profiles from which melting temperatures were deduced. One- and two-exponential least-squares fits on kinetic data were carried out with the MINSQ program of Micromath (Salt Lake City, UT).

CD (circular dichroic) spectra were measured by a Jasco J-500A recording spectropolarimeter using water-jacketed cylindrical cells of 2-cm path length. CD kinetic measurements were made by monitoring ellipticity changes at 287 nm for both association and SDS-induced dissociation. Fluorescence kinetic measurements were made with an SLM 48000S spectrofluorometer by monitoring emissions at 566 nm with 448-nm excitations. Electrophoretic measurements were made on a Pharmacia Phast System using 20% polyacrylamide gels at 200 V with appropriate pre- and postloading run times at different temperatures. PhastGel native buffer strips containing 0.25 M Tris of pH 8.8 were used, and the gels were developed by silver staining.

RESULTS

Relative Tetranucleotide Sequence Specificities of CHR As Revealed by Absorption Spectral Comparison. CHR exhibits an absorbance maximum at 406 nm when free in solutions. Successive additions of DNA lead to progressive bathochromic shifts and intensity enhancements at 440 nm and a concomitant reduction at the 400-nm region (Hayasaka & Inoue, 1969). A typical absorption spectral titration of CHR with d(GTA-GGCC-TAC) is shown in Figure 1. An isosbestic point is clearly evident at 411 nm, suggesting a two-component process. Thus, absorbance changes at a given wavelength or absorbance differences at two wavelengths can be used to construct binding isotherms and to obtain binding parameters (see later). However, qualitative ranking of the relative binding affinity of CHR with different sequences can be achieved by simply comparing the intensity enhancements of CHR absorbance around 440 nm in the presence of various oligomers of the same concentration.

Comparison of absorption difference spectra (not shown) of 5 μM CHR in the presence and in the absence of 50 μM oligomers indicates that the decamer containing the -GGCC- sequence induces the largest spectral changes at the 440-nm region. Second in line is the -CGCG- sequence, closely followed by -GCGC- and -CCGG- which exhibit nearly identical spectral changes. Despite the presence of only two contiguous G·C base pairs, -AGCT- exhibits significant CHR affinity as evidenced by the considerable spectral changes. The sequences -ACGT-, -TGCA-, and -TCGA- in that order induce progressively less spectral changes. Thus, these qualitative difference spectral comparisons establish the following CHR binding order: GGCC > CGCG > GCGC, CCGG > AGCT > ACGT, TGCA > TCGA.

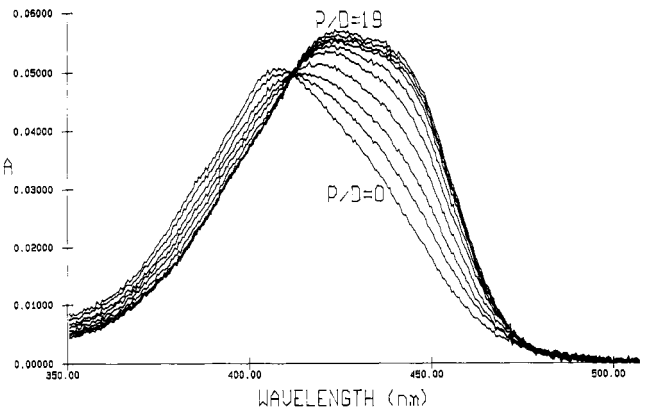

FIGURE 1: Representative absorption spectral titration as typified by progressively adding the d(GTA-GGCC-TAC) stock to a 5 μM CHR solution at 25 °C. Each spectrum was taken after a 12-min wait to ensure equilibrium, as the association kinetics are relatively slow. P/D designates [DNA, per base]/[drug] ratio. All spectra were normalized to 5 μM CHR.

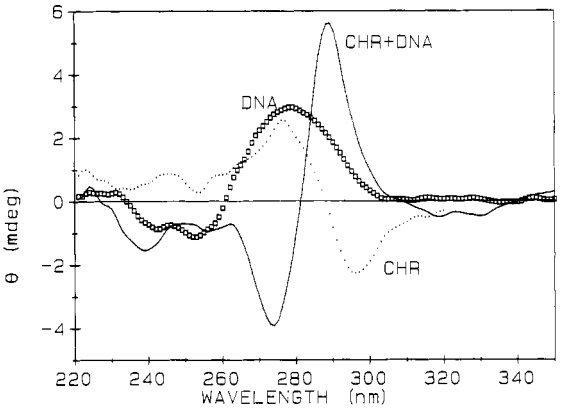

FIGURE 2: Comparison of CD spectra of a 5 μM CHR solution and 40 μM d(GTAGGCCTAC) solutions in the absence and in the presence of 5 μM CHR. Measurements were made at room temperature using a cylindrical cell of 2-cm path length.

CD Measurements Support the Proposed Binding Order. CHR is optically active and exhibits negative and positive CD maxima at 295 and 276 nm, respectively. However, in the presence of DNA, a strong exciton-type couplet, presumably the result of dimer formation and/or aglycon–DNA base interactions, is induced which results in an inverted CD spectrum with positive and negative maxima appearing at 287 and 275 nm, respectively (Dalgleish et al., 1974). This can clearly be seen in Figure 2 where the CD spectra of CHR, d(GTA-GGCC-TAC), and CHR+oligomer are compared. Thus, induced CD intensities at 287 and 275 nm can serve as gauges for the relative binding affinities of CHR toward these oligomers. CD difference spectra of CHR in the presence and in the absence of decamers containing four central G·C base pairs are compared in the top panel of Figure 3. Supporting the absorbance results, -GGCC- induces the largest CD intensity changes at 287 nm and does so even more dramatically at 275 nm. On the other hand, CD intensity changes of -CGCG- are significantly less. Those of -GCGC- and -CCGG- are nearly identical but are measurably less than those of -CGCG-. CD difference spectra for sequences

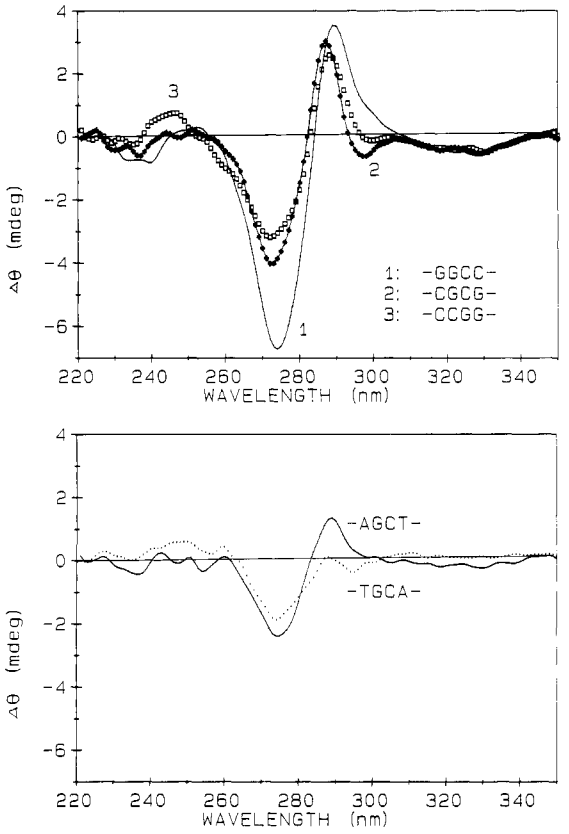

FIGURE 3: Comparison of difference CD spectra of 40 μM DNA in the presence and absence of 5 μM CHR. (Top) For decamers containing four contiguous G·C base pairs. The difference CD spectrum for -GCGC- is nearly identical to that of -CCGG- and is not shown. (Bottom) For the -AGCT- and -TGCA-containing decamers.

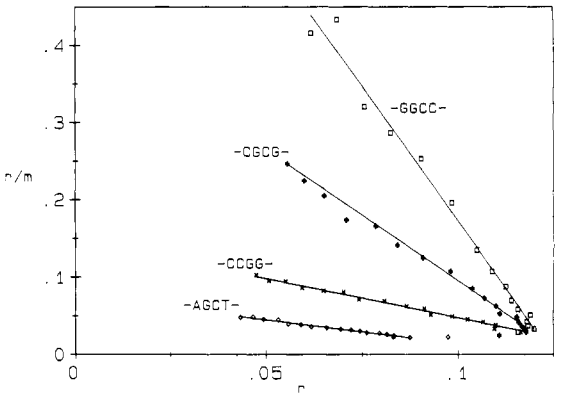

FIGURE 4: Representative Scatchard plots at 25 °C for some of the decamers studied. Absorbance differences between those of 440 and 400 nm are used to construct the binding isotherms. Solid lines are those of linear least-squares fits to the simple Scatchard equation $r/m = K_a(n - r)$, where r is the ratio of bound drug to DNA base concentrations, n is the saturation binding density, K_a is the apparent association constant, and m is the free drug concentration.

Table 1: Summary of Binding Parameters for Chromomycin A_3 at 25 °C

	Scatchard parameters		model fits	
oligomer	K_a (μM^{-1})	n(drug/duplex)	K_2 (μM^{-2})	K_L (μM^{-1})
d(GTA-GGCC-TAC)	7.0	2.5	3.3	67
d(GTA-CGCG-TAC)	3.3	2.6	1.3	420
d(GTA-GCGC-TAC)	1.0	2.7	0.7	790
d(GTA-CCGG-TAC)	1.0	2.9	0.8	940
d(GTA-AGCT-TAC)	0.6	2.4	0.2	2
d(GTA-TGCA-TAC)	~0.2		0.06	7
d(GTA-ACGT-TAC)	~0.3		0.04	13
d(GTA-TCGA-TAC)	<0.1			

containing -AGCT- and -TGCA- are compared in the bottom panel of Figure 3. Appreciable differences are observed for these two sequences, with -AGCT- inducing considerably larger spectral changes upon drug complexation. The sequence -ACGT- (not shown) induces spectral changes at 287 nm which are significantly smaller than those of -AGCT- but slightly larger than that of -TGCA-. The negligible CHR binding of the -TCGA- sequence is apparent from the presence of negative bands at 295 nm (not shown), characteristic of free CHR in solutions (see Figure 2). These results are consistent with the binding order established via absorbance results.

Elucidation of Binding Parameters via Absorption Spectral Titration. To gain more quantitative binding information, absorption spectral titrations were carried out at 25 °C. Absorbance differences at 440 and 400 nm were used to obtain the binding isotherms and representative Scatchard plots which are shown in Figure 4. Since the plots can be approximated by straight lines, the binding parameters were deduced via linear least-squares fits. The results are summarized in Table 1. As can be seen, the decamer with -GGCC- exhibits the highest CHR affinity with a binding constant of 7.0 μM^{-1}. This is followed by -CGCG- which has value of 3.3 μM^{-1}. Binding constants for both -CCGG- and -GCGC- are about 1.0 μM^{-1}. That of -AGCT- is slightly lower at 0.6 μM^{-1}, and those of -ACGT- and -TGCA- are approximately 0.3 and 0.2 μM^{-1}, respectively. The binding constant of -TCGA- is considerably lower than 0.1 μM^{-1}. All binding densities were estimated to be between two and three drug molecules per duplex, which is in general agreement with the drug dimer binding at a single site. Thus, our quantitative binding constant estimations are consistent with the relative binding order deduced via qualitative spectral comparisons.

To obtain reliable binding parameters via Scatchard plots, reasonable estimates of the extinction coefficients for the bound drugs are essential. This, however, is not always possible, especially for the weaker binding complexes. An additional complication arises from potential hairpin formation in our self-complementary oligomers in dilute solutions used in optical studies. Thus, attempts were also made to fit the experimental binding isotherms with the following binding model, assuming only the hairpin (L) and dimeric duplex (L_2) coexist in solutions with equilibrium constant K_L and only duplex binds to CHR (X) in a 1 (duplex):2 (drug) ratio with a binding constant K_2:

$$2L \overset{K_L}{\rightleftharpoons} L_2 \qquad 2X + L_2 \overset{K_2}{\rightleftharpoons} X_2L_2$$

Mass balances of drug and DNA result in

$$[X] = [L] + 2K_L[L]^2 + X_t - L_t$$

$$L_t = [L] + 2K_L[L]^2 + 2K_2K_L[X]^2[L]^2$$

$$A = \epsilon_f[X] + 2\epsilon_bK_2K_L[X]^2[L]^2$$

where A is the measured absorbance, ϵ_f and ϵ_b are the extinction coefficients of free and bound drugs, respectively, and X_t and L_t are the total drug and DNA strand concentrations, respectively. Nonlinear least-squares fits for our titrations are compared with the experimental data in Figure 5 and the fitted parameters included in Table 1. As is apparent, satisfactory fits, especially those of weaker binding oligomers, are obtained, and the extracted parameters appear to be quite reasonable. Again, the binding constants are consistent with

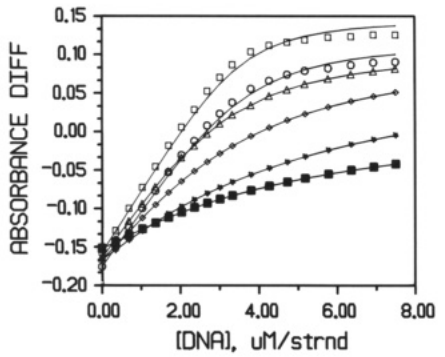

FIGURE 5: Comparison of experimental binding isotherms with their nonlinear least-squares fitted curves (solid curves) using the model described in the text: d(GTA-GGCC-TAC) (open squares); -CGCG- (open circles); -GCGC- (triangles); -AGCT- (diamonds); -ACGT- (stars); and -TGCA- (solid squares). Data for -CCGG- are not shown, as they are nearly identical to those of -GCGC-.

Table 2: Comparison of Melting Temperatures of Oligomers and Their Increases upon CHR Binding

oligomer	t_m (°C)	Δt_m (°C)
d(GTA-GGCC-TAC)	44	11
d(GTA-CGCG-TAC)	45	11
d(GTA-GCGC-TAC)	45	5
d(GTA-CCGG-TAC)	44	5
d(GTA-AGCT-TAC)	33	7
d(GTA-TGCA-TAC)	34	5
d(GTA-ACGT-TAC)	35	4
d(GTA-TCGA-TAC)	34	1

Table 3: Summary of Association and Dissociation Rates of CHR at 25 °C

oligomer	k_a (min^{-1})	k_d (min^{-1})
d(GTA-GGCC-TAC)	0.61	0.031
d(GTA-CGCG-TAC)	0.67	0.036
d(GTA-GCGC-TAC)	0.69	0.46
d(GTA-CCGG-TAC)	0.57	0.29
d(GTA-AGCT-TAC)	0.77	0.49
d(GTA-ACGT-TAC)	0.80	1.9
d(GTA-TGCA-TAC)	0.74	11
d(GTA-TCGA-TAC)	0.74	>2

the order established by other means. It is also gratifying to note that the duplex formation constants from the hairpin are considerably larger for decamers with four central G·C base pairs than those with two, as expected.

CHR Binding Stabilizes the DNA Duplex. DNA melting measurements were carried out to investigate the effect of CHR binding on DNA duplex stability. Except for the -TCGA- oligomer, measurable melting temperature increases were observed for the decamers upon CHR binding, and the results are summarized in Table 2. The extent of melting temperature increase appears to be in general agreement with that of the proposed relative binding affinity. Indeed, the -GGCC- and -CGCG- oligomers exhibit the largest melting temperature increases of about 11 °C.

Association and Dissociation Kinetic Measurements. Association kinetic measurements were carried out by adding the DNA stocks to the CHR solutions to result in drug and DNA concentrations of 4.85 and 40 μM, respectively. Time-dependent absorbance changes at 440 nm were monitored. The observed data can be adequately approximated by single-exponential decays, since the two-exponential fits did not result in significant improvements in the sum of square deviations. The fitted rate constants k_a are summarized in Table 3. As is apparent, no significant differences in the association rates were observed among the oligomers studied, and they range

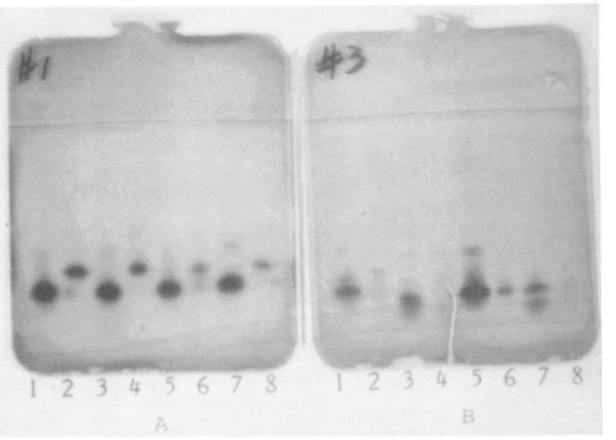

FIGURE 6: Comparison of electrophoretic mobility patterns at 14 °C for decamers in the absence and in the presence of CHR. (A) 1 mM d(GTA-GGCC-TAC) (lane 1), d(GTA-CGCG-TAC) (lane 3), d(GTA-GCGC-TAC) (lane 5), and d(GTA-CCGG-TAC) (lane 7); lanes 2, 4, 6, and 8 are the corresponding oligomers in the presence of 150 μM CHR. (B) 1 mM d(GTA-AGCT-TAC) (lane 1), d(GTA-TGCA-TAC) (lane 3), d(GTA-ACGT-TAC) (lane 5), and d(GTA-TCGA-TAC) (7); lanes 2, 4, 6, and 8 are the corresponding oligomers in the presence of 150 μM CHR.

from 0.6 to 0.8 min^{-1}. Total absorbance changes at 440 nm via pre- and postreaction spectral measurements (not shown) are consistent with the earlier suggested binding orders.

Dissociation kinetics were measured by adding 20% SDS stocks to the CHR–DNA solutions to result in 1% SDS. Time-dependent absorbances at 340 nm and emission intensities at 566 nm with 448-nm excitation were monitored. Dissociation rate constants were obtained via single-exponential least-squares fits, and the averages of absorbance and fluorescence measurements are included in Table 3. Contrasting the association kinetics, however, dramatic variation in the rates of drug dissociation from oligomers is apparent. Strikingly slow SDS-induced CHR dissociations from the -GGCC- and -CGCG- oligomers were observed which are nearly an order of magnitude slower than from -GCGC- and -CCGG-. Also noteworthy is the fact that CHR not only dissociates from -AGCT- more slowly than from -ACGT- but also dissociated significantly slower than from -TGCA-. The trend exhibited by the dissociation rates is consistent with the suggested binding order established via equilibrium studies.

Electrophoretic Evidence on CHR–DNA Complex Formation. Gel electrophoretic mobilities of oligomers in the absence and in the presence of CHR are shown in Figure 6. As can be seen in panel A, all four decamers containing four central G·C base pairs exhibit retarded bands upon drug complexation. The intensities of the retarded bands for the -GCGC- and -CCGG- oligomers, however, are considerably less intense than those of -GGCC- and -CGCG-. These results are consistent with their weaker binding and faster dissociation rates. The decamers containing only two central G·C base pairs are shown in panel B, and only the -AGCT- oligomer exhibits a visible retarded band but its intensity is somewhat weaker than those of -GCGC- and -CCGG-. This is consistent with the significant CHR binding affinity of the -AGCT- sequence and the still weaker binding affinities of the other three oligomers.

DISCUSSION

Absorption and CD spectral evidence indicates that the CHR binding affinities of the self-complementary tetranucleotide sequences containing at least two contiguous G·C

base pairs are in the following order: -GGCC- > -CGCG- > -GCGC-, -CCGG- > -AGCT- > -ACGT-, -TGCA- > -TCGA-. The general relative binding order is supported by gel retardation, thermal denaturation, and dissociation kinetic measurements. The SDS-induced drug dissociation from the -GGCC- and -CGCG-containing oligomers is found to be more than an order of magnitude slower than the rest of the sequences studied. The considerably weaker binding of -GCGC-, -CCGG-, and -ACGT-, each containing a central 5′CG3′ step, as compared to the corresponding sequence isomers -GGCC-, -CGCG-, and -AGCT-, each containing a central 5′GC3′ step, is consistent with the preference of CHR to the GC step. However, CHR binding is seen to be strongly modulated by the adjacent base pairs or sequences. For example, despite the presence of a central GC step, CHR binding to -AGCT- is significantly weaker and dissociation occurs considerably faster than -GGCC- and -CGCG-. This is further exemplified by -TGCA- which exhibits a much weaker affinity for the drug.

Thus, our results support the earlier NMR findings (Gao & Patel, 1989; Gao et al., 1992) which suggest the sequence-specific binding of CHR to the 5′GC3′ sequence. The strong preference for the GC step has been attributed to the head to tail dimer orientation of CHR at the widened and shallower minor groove binding site and is associated with specific intermolecular hydrogen bond formations of the OH group at the C8 of aglycon with NH_2 and N3 of guanine. Furthermore, the stronger binding of -GGCC- and -CGCG- as compared to -AGCT- may be understood in terms of the additional hydrogen bonding capability of the E sugar ring with the 2-amino group of the guanine adjacent to the central GC step (Gao et al., 1992). The much weaker binding of -TGCA- as compared to -AGCT-, however, is not clear and may have its origin in sequence-dependent conformational differences (such as groove width) and/or sugar rings and minor groove interactions.

It should be noted that the binding preference of GC over CG has also been demonstrated by Banville et al. (1990). Their NMR studies revealed strong CHR binding to d(ATGCAT), d(TATGCATA), and d(ATAGCTAT) but not to d(ATCGAT). The negligible binding of CHR to d(ATCGAT) is consistent with our finding that -TCGA- is the weakest binding sequence. Yet, our results which show weak binding of CHR to d(GTA-TGCA-TAC) differ from the finding of Banville et al. that d(ATGCAT) and d(TATGCATA) bind strongly. Although the basis for such a discrepancy is not clear, it is unlikely to be the consequence of sequence-dependent conformational differences, as our oligomer encompasses both their sequences. However, one cannot rule out the possibility of a significant contribution from the nonbinding hairpin form in our less concentrated optical studies. Such contributions would likely affect both d(GTA-AGCT-TAC) and d(GTA-TGCA-TAC) to a similar extent, as shown by the similar gel electrophoretic patterns (not shown) and the nearly identical duplex melting temperatures of these two sequence isomers (see Table 2). Thus, our finding of significant CHR affinity for -AGCT- but not for -TGCA- suggests that hairpin formation may not be the main culprit for weak CHR binding to d(GTA-TGCA-TAC), although hairpin formation most certainly is partially responsible for the observed weaker CHR binding to -AGCT- than to -GGCC- and -CGCG-.

Our finding of large variation in dissociation rates among different sequences is significant. The fact that CHR dissociates from -GGCC- and -CGCG- more than an order of magnitude slower than from -AGCT- and -TGCA- suggests that the G·C base pairs adjacent to the strong binding GC step may be involved in hydrogen bonding and are responsible for the observed much slower dissociation kinetics. As mentioned earlier, such hydrogen bonds were in fact observed in the CHR+d(AAGGCCTT) system (Gao et al., 1992) between E pyranose rings and the adjacent G·C base pairs. Leroy et al. (1991) recently extended the CHR–d(AAGGCCTT) structural studies to include hydrogen exchange measurements. It was found that the opening rate of the four central base pairs, which interact with CHR in the complex, is less than that of the free duplex by 1–2 orders of magnitude. Leroy and associates used the proton–deuterium exchange rate to estimate a complex dissociation time of around 60 h at 25 °C; a comparison between our results, however, is not straightforward because the SDS employed by us facilitates drug dissociation.

It is also interesting to compare the dissociation kinetics of CHR with those of actinomycin D (ACTD) which is also GC sequence specific but is intercalative in nature. For example, the SDS-induced CHR dissociation from d(GTA-GGCC-TAC) exhibits a characteristic time of about 32 min at 25 °C which is comparable to the single characteristic time of 55 min for ACTD dissociation from d(ATATGCATAT) at 18.5 °C (Chen, 1988). The slow dissociation kinetics exhibited by both drugs are no doubt related to the abilities of both chromophores to hydrogen bond to the central G·C base pairs and favorable side chain interactions with the minor groove. In contrast to the hydrogen bonding abilities of pyranose side chains of CHR, the pentapeptide ring interactions of ACTD with the minor groove are more hydrophobic in nature. This results in the preference of A·T adjacent base pairs, with -TGCA- becoming a strong binding and slow dissociation sequence (Chen, 1988). The strong dependence of dissociation rates on binding sequences also suggests that the observed multiple-exponential dissociation kinetics of CHR from native DNA (Behr et al., 1969) may likely be adequately described by the site-heterogeneity model, similar to that of ACTD (Krugh et al., 1980; Chen, 1988).

Although no significant variation in the rates of association was found among the sequences studied, the observed rate constants of 0.6–0.8 min^{-1} are worth commenting on. The characteristic association times of more than 1 min are considerably slower than for most other drugs. Such slow processes may originate from the requirement for widening of the minor groove to accommodate the bulky drug dimer and properly positioning the chromophores and side chains for optimal interactions. This appears to be supported by a rudimentary study indicating the absence of significant association rate alterations despite a 10-fold change in either CHR or DNA concentration.

Our spectral titrations yielded a binding constant of 7×10^6 M^{-1} at 25 °C for CHR binding to d(GTA-GGCC-TAC). Recently, Stankus et al. (1992) conducted a quantitative footprinting analysis of CHR with an 18-mer duplex and estimated a binding constant of $(2.7 \pm 1.4) \times 10^7$ M^{-1} at 37 °C for a -TGGCCA- site. Although an increase in binding affinity is to be expected for a longer oligomer, the differing techniques, concentrations, and experimental conditions made a meaningful comparison between our value and theirs difficult.

Our finding of a duplex stabilization effect upon CHR binding is also of interest, since earlier studies either indicated no duplex stabilization effect (Kersten et al., 1966) or indicated a significant melting temperature increase (Kajiro & Kamiyama, 1967) upon CHR binding to native DNA. Again, the larger melting temperature increases for the stronger

binding sequences are likely the consequence of the additional hydrogen bonding capability of these sequences.

As our studies have been restricted to the self-complementary tetranucleotide sequences, correlation with the trinucleotide sequence specificity from footprinting experiments is not straightforward and, consequently, not attempted.

Finally, a recent single-crystal X-ray analysis of d(CATGGCCATG) has revealed a smooth bend of 23° over the central four base pairs in a direction that compresses the wide major groove of the double helix (Goodsell et al., 1993). As -GGCC- has been found to be the strongest CHR binding site at the self-complementary tetranucleotide level, it is tempting to speculate that such a bend may have resulted in a better fit for the Mg^{2+}-mediated drug dimer in the minor groove of this particular sequence. Our laboratory, however, does not have the graphic modeling capability to verify such a speculation.

ACKNOWLEDGMENT

We thank D. Dunson for her careful reading of the manuscript.

REFERENCES

Banville, D. L., Keniry, M. A., & Shafer, R. H. (1990) *Biochemistry 29*, 9294–9304.
Behr, W., & Hartman, G. (1965) *Biochem. Z. 343*, 519–527.
Behr, W., Honikel, K., & Hartmann, G. (1969) *Eur. J. Biochem. 9*, 82–92.
Chen, F.-M. (1988) *Biochemistry 27*, 6393–6397.
Cons, B. M. G., & Fox, K. R. (1989a) *Nucleic Acids Res. 17*, 8695–8714.
Cons, B. M. G., & Fox, K. R. (1989b) *Nucleic Acids Res. 17*, 5447–5459.
Cons, B. M. G., & Fox, K. R. (1991) *Biochemistry 30*, 6314–6321.
Dalgleish, D. G., Fey, G., & Kersten, W. (1974) *Biopolymers 13*, 1757–1766.
Dasgupta, D., Shashiprabha, B. K., & Podder, S. K. (1979) *Ind. J. Biochem. Biophys. 16*, 18–21.
Fasman, G. D. Ed. (1975) *CRC Handbook of Biochemistry and Molecular Biology*, 3rd ed., Vol. I, p 589, Chemical Rubber Publishing Co., Cleveland, OH.
Fox, K. R., & Howarth, N. R. (1985) *Nucleic Acids Res. 13*, 8695–8714.
Gao, X., & Patel, D. J. (1989) *Biochemistry 28*, 751–762.
Gao, X., & Patel, D. J. (1990) *Biochemistry 29*, 10940–10956.
Gao, X., Mirau, P., & Patel, D. J. (1992) *J. Mol. Biol. 223*, 259–279.
Goldberg, I. H., & Friedman, P. A. (1971) *Annu. Rev. Biochem. 40*, 775–810.
Goodsell, D. S., Kopka, M. L., Cascio, D., & Dickerson, R. E. (1993) *Proc. Natl. Acad. Sci. U.S.A. 90*, 2930–2934.
Hayasaka, T., & Inoue, Y. (1969) *Biochemistry 8*, 2342–2347.
Kaziro, Y., & Kamiyama, M. (1967) *J. Biochem. (Tokyo) 62*, 424–429.
Keniry, M. A., Brown, S. C., Berman, E., & Shafer, R. H. (1987) *Biochemistry 26*, 1058–1067.
Kersten, W., Kersten, H., & Szybalski, W. (1966) *Biochemistry 5*, 236–244.
Krugh, T. R., Hook, J. W., Balakrishnan, M. S., & Chen, F.-M. (1980) in *Nucleic Acids Geometry and Dynamics* (Sarma, R. H., Ed.) pp 351–366, Pergamon, New York.
Leroy, J. L., Gao, X., Gueron, M., & Patel, D. J. (1991) *Biochemistry 30*, 5653–5661.
Muller, W., & Crothers, D. M. (1968) *J. Mol. Biol. 35*, 251–290.
Prasad, K. S., & Nayak, R. (1976) *FEBS Lett. 71*, 171–174.
Sarker, M., & Chen, F.-M. (1989) *Biochemistry 28*, 6651–6657.
Sastry, M., & Patel, D. J. (1993) *Biochemistry 32*, 6588–6604.
Stankus, A., Goodisman, J., & Dabrowiak, J. C. (1992) *Biochemistry 31*, 9310–9318.
Van Dyke, M. W., & Dervan, P. B. (1983) *Biochemistry 22*, 2373–2377.
Ward, D. C., Reich, E., & Goldberg, I. H. (1965) *Science 149*, 1259–1263.
Waring, M. J. (1970) *J. Mol. Biol. 54*, 247–279.